Journal of Marine Science and Application (2019) 18:195–204
https://doi.org/10.1007/s11804-019-00093-7

RESEARCH ARTICLE

Synchrophasing Vibration Control of Machines Supported by Discrete Isolators

Di Huang[1] · Tiejun Yang[1] · Zhigang Liu[1] · Michael J. Brennan[2] · Xinhui Li[1]

Received: 11 October 2018 / Accepted: 25 March 2019 / Published online: 6 June 2019

Abstract
This paper describes an analytical investigation into synchrophasing, a vibration control strategy on a machinery installation in which two rotational machines are attached to a beam-like raft by discrete resilient isolators. Forces and moments introduced by sources are considered, which effectively represent a practical engineering system. Adjusting the relative phase angle between the machines has been theoretically demonstrated to greatly reduce the cost function, which is defined as the sum of velocity squares of attaching points on the raft at each frequency of interest. The effect of the position of the machine is also investigated. Results show that altering the position of the secondary source may cause a slight change to the mode shape of the composite system and therefore change the optimum phase between the two machines. Although the analysis is based on a one-dimensional Euler–Bernoulli beam and each machine is considered as a rigid-body, a key principle can be derived from the results. However, the factors that can influence the synchrophasing control performance would become coupled and highly complicated. This condition has to be considered in practice.

Keywords Discrete supported machines · Vibration isolation · Raft · Synchrophasing control · Different forms of excitations

1 Introduction

The vibration and noise introduced by marine machines can significantly affect the safety of ships, reliability of equipment aboard, and comfort of passengers. For military ships, the noise caused by low-frequency vibration can be particularly harmful because it reduces the acoustic stealth of the ships. With the development of a lightweight and large-scale hull structure, the vibration and noise control has become increasingly important.

Passive vibration isolators are widely employed to isolate sources, such as rotational machines, from host structures to reduce transmitted vibration. However, when different configurations are used, such as a floating raft isolation, traditional passive isolators involve a tradeoff between the efficiency of the isolation performance and the stability of the entire system. To solve this problem, active vibration control has been proposed, which introduces secondary sources to generate forced vibration responses to cancel the primary vibration transmission (Fuller et al. 1997; Yang et al. 2004). However, a back-up system is always needed no matter what kind of actuators are used, thereby necessitating space and cost. Furthermore, the control algorithm used in the process may diverge when the vibration level changes substantially in a short time, thus increasing the vibration.

As an alternative control method, synchrophasing is considered in this study. The principle of synchrophasing is not complicated and is based on the idea of reducing the vibrations originating from two engines of a steam ship by making the two engines run at the same speed but in anti-phase (Mallock 1905). Synchrophasing has been widely developed for noise control in aircraft cabins (Fuller 1986) rather than for

Article Highlights
- A realistic analytical model of the machinery raft system is presented and compared with a numerical model, which is used to investigate the synchrophasing control method.
- The influence of the moment introduced by the machines to the performance of the synchrophasing is studied.
- The effect of the machine's position on the optimum phase is investigated.

✉ Tiejun Yang
yangtiejun@hrbeu.edu.cn

[1] College of Power and Energy Engineering, Harbin Engineering University, Harbin 150001, China

[2] Departamento de Engenharia Mecânica, UNESP, St. Paul 03001-000, Brazil

vibration control. Harada (1977) obtained a patent for a technique to reduce the blade passage tonal noise of two fans in a duct by adjusting the relative angle between the two sets of fan blades. Howard (2004) demonstrated experimentally that synchrophasing can reduce the sound pressure level by 10 dB at the blade passage frequency or its harmonics. Subsequently, several studies on noise control in aircraft cabins (Jones and Fuller 1986; Efimtsov and Zverev 1992) were published and two patents were registered for techniques to reduce sound and/or vibration on multiple rotating machines (Pla and Goodman 1993, Pla 1998) by adjusting the phase angle between the propellers or machines. The research also extended to active synchrophasing. For example, microphones and accelerometers were positioned throughout an aircraft cabin to detect error signals in some adaptive algorithms that were used to determine the optimum phase angle to minimize the cabin noise and vibration over a wide range of flight conditions (Magliozzi 1995; Blunt and Rebbechi 2007; Huang et al. 2015).

Only a few studies have been conducted on controlling vibration transmission from a machinery raft to a host structure by adjusting the phase angles between the machines. Several articles only discuss the effect of the phase angle between two machines installed on a raft (Song and Yu 2008; Fu et al. 2012; Li 2015). Recent research by Dench et al. (2013) on synchrophasing demonstrated the principle of this method on a 1D structure. The researchers considered theoretically the behavior of a machinery raft, and conducted an experimental study to illustrate the application of synchrophasing to multiple machines for a marine application. Yang et al. (2018) subsequently investigated the effectiveness of the control strategy in the marine environment through an experimental study. A large-scale floating raft system supported on a hull-like structure located in a laboratory setting was considered. Each machine was driven by a phase asynchronous motor and had two counter rotating shafts with adjustable eccentric masses, which allowed the dynamic force generated by each machine to be set independently. To reduce the vibration transmitted to the hull-like structure, the electrical supply to the motors was adjusted by a synchrophasing control scheme, which used a genetic algorithm to determine the optimum phases between the machines.

To simplify the detailed analysis, the application of synchrophasing to vibration control is investigated on a 1D structure used as the machinery raft, while each source is assumed to be a smaller beam and supported by passive isolators at each end. In this case, both forces and moments introduced by the sources are considered, which effectively represents a practical engineering system. The effect of the position of the machines is investigated using a numerical model. The critical feature of the effect of various factors can be determined although the situation would be more complex in real applications.

2 Description of Isolation System

2.1 Model of Analysis Structure

Figure 1 presents the typical marine machinery installation, which consists of machines, resilient mounts, floating raft, and the ship body.

The idealized model used to investigate and determine the performance of synchrophasing and the effect of position of the sources is shown in Fig. 2. Two synchronous machines are resiliently attached to a long raft, which is supported by two identical elastic springs at the ends. The machines can be considered as rigid bodies; therefore, only the displacement and rotation of each machine should be considered. Previous work (Dench et al. 2013) had investigated harmonic sources, representative of rotating machines, where the sources were directly applied to a receiving structure in a translational direction only and the sources were not distributed but acted at single point.

To be realistic, the raft should be considered as flexible, which can be represented as a free–free beam shown in Fig. 3. The beam subsystem has six external forces f_i ($i = 1$–6) acting on it at six points marked as x_i ($i = 1$–6). The displacements at the six positions denoted by w_i ($i = 1$–6) can be represented by the following equation (Dench et al. 2005):

$$\begin{Bmatrix} w_1 \\ w_2 \\ w_3 \\ w_4 \\ w_5 \\ w_6 \end{Bmatrix} = \begin{bmatrix} \beta_{11} & \beta_{12} & \beta_{13} & \beta_{14} & \beta_{15} & \beta_{16} \\ \beta_{21} & \beta_{22} & \beta_{23} & \beta_{24} & \beta_{25} & \beta_{26} \\ \beta_{31} & \beta_{32} & \beta_{33} & \beta_{34} & \beta_{35} & \beta_{36} \\ \beta_{41} & \beta_{42} & \beta_{43} & \beta_{44} & \beta_{45} & \beta_{46} \\ \beta_{51} & \beta_{52} & \beta_{53} & \beta_{54} & \beta_{55} & \beta_{56} \\ \beta_{61} & \beta_{62} & \beta_{63} & \beta_{64} & \beta_{65} & \beta_{66} \end{bmatrix} \begin{Bmatrix} f_1 \\ f_2 \\ f_3 \\ f_4 \\ f_5 \\ f_6 \end{Bmatrix} \quad (1)$$

where $$\beta_{ij}(\omega) = \frac{1}{-m_b\omega^2} + \frac{3\left(1-2\frac{x_i}{L}\right)\left(1-2\frac{x_j}{L}\right)}{-m_b\omega^2} + \sum_{k=1}^{\infty} \frac{W_k(x_i)W_k(x_j)}{m_{m,k}\left(\omega_k^2(1+i\eta)-\omega^2\right)}$$

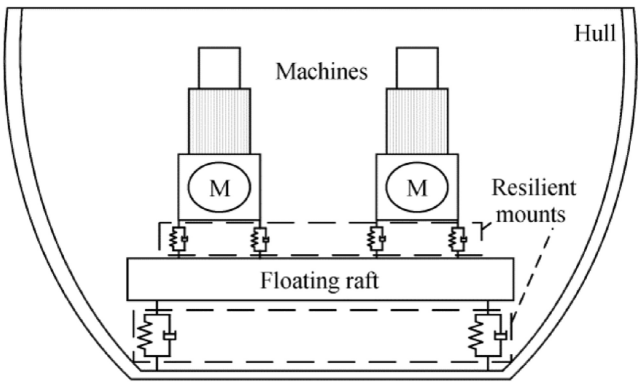

Fig. 1 Typical marine machinery installation

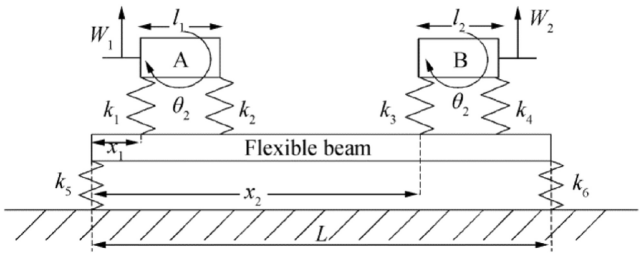

Fig. 2 Model and parameters of system. Two machines are resiliently mounted on a rigid beam of which the ends are supported by springs

is the receptance of the free–free Euler–Bernoulli beam, that is the displacement at position x_i due to the force acting on the beam at position x_j, m_b is the mass of the beam while $m_{m,k}$ denotes the kth modal mass, $W_k(x)$ is the mode shape of the kth flexural mode of the free–free beam at the kth natural frequency given by ω_k, and η is the modal structural loss factor that is assumed to be constant for all modes. Equation (1) can be written in vector matrix form as

$$\boldsymbol{w}_b = \boldsymbol{Y}\boldsymbol{f}_{\text{beam}} \tag{2}$$

where $\boldsymbol{w}_b$ is the vector of displacement, $\boldsymbol{Y}$ is the receptance matrix, and $\boldsymbol{f}_{\text{beam}}$ is the vector of excitation forces.

The six external forces are actually internal forces that are introduced by the attached components in the entire system. In this situation, the force vector

$$\boldsymbol{f}_{\text{beam}} = f_1 \;\; f_2 \;\; f_3 \;\; f_4 \;\; f_5 \;\; f_6{}^{\text{T}}$$

becomes

$$\boldsymbol{f}_{\text{beam}} = \left\{ \begin{array}{cc} k_1\left(w_{I_1 l}^t - w_{I_1 l}^b\right) & k_2\left(w_{I_1 r}^t - w_{I_1 r}^b\right) \\ k_3\left(w_{I_2 l}^t - w_{I_2 l}^b\right) & k_4\left(w_{I_2 r}^t - w_{I_2 r}^b\right) \\ -k_5 w_l - k_6 w_r & \end{array} \right\}^{\text{T}} \tag{3}$$

where $w_{I_i l}^t$ and $w_{I_i r}^t$ ($i = 1$ or 2) indicate the displacements of the top ends of the left or right mounts that connect the ith machine to the raft. The displacements of the bottom ends of the left or right mounts are represented by $w_{I_i l}^b$ and $w_{I_i r}^b$ ($i = 1, 2$),

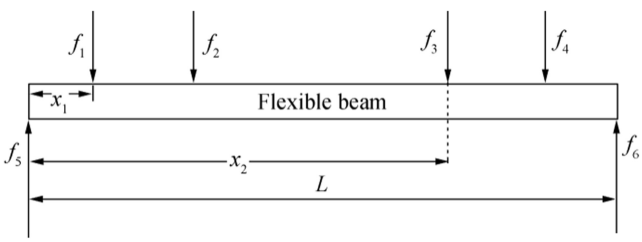

Fig. 3 Separated beam subsystem on which the machine positions are marked as x_1 and x_2, respectively

respectively; w_l and w_r denote the displacements of the mounts supporting the raft on its two ends separately; and k_1, k_2, k_3, k_4, k_5, and k_6 are the stiffness of the springs connected between the machine masses and the host structure and between the raft and the fixed ground.

By using compatibility condition, which requires the displacement of each attaching point to be the same, Eq. (3) can be rewritten as

$$\boldsymbol{f}_{\text{beam}} = \left\{ \begin{array}{c} k_1\left[\left(w_{M_1} - \frac{l_1}{2}\theta_{M_1}\right) - w_1\right] \\ k_2\left[\left(w_{M_1} + \frac{l_1}{2}\theta_{M_1}\right) - w_2\right] \\ k_3\left[\left(w_{M_2} - \frac{l_2}{2}\theta_{M_2}\right) - w_3\right] \\ k_4\left[\left(w_{M_2} + \frac{l_2}{2}\theta_{M_2}\right) - w_4\right] \\ -k_5 w_5 \\ -k_6 w_6 \end{array} \right\} = \left\{ \begin{array}{c} \boldsymbol{K}_{I_1}\left(-\boldsymbol{R}_1^{\text{T}}\boldsymbol{x}_1 - \boldsymbol{w}_{I_1}\right) \\ \boldsymbol{K}_{I_2}\left(-\boldsymbol{R}_2^{\text{T}}\boldsymbol{x}_2 - \boldsymbol{w}_{I_2}\right) \\ \boldsymbol{K}_S\left(-\boldsymbol{w}_S\right) \end{array} \right\} \tag{4}$$

where $\boldsymbol{K}_{I_1} = \begin{bmatrix} k_1 & 0 \\ 0 & k_2 \end{bmatrix}$ and $\boldsymbol{K}_S = \begin{bmatrix} k_5 & 0 \\ 0 & k_6 \end{bmatrix}$ are the stiffness matrix of the isolators for the two machines and the raft, respectively; $\boldsymbol{R}_i = \begin{bmatrix} -1 & -1 \\ \frac{l_i}{2} & -\frac{l_i}{2} \end{bmatrix}$ ($i = 1, 2$) is the transfer matrix in which l_1 and l_2 are the lengths of the two machines; $\boldsymbol{x}_i = \{ w_{M_i} \quad \theta_{M_i} \}^{\text{T}}$ ($i = 1, 2$) is the vector of the movements of the machines; $\boldsymbol{w}_{I_1} = \{ w_1 \quad w_2 \}^{\text{T}}$, $\boldsymbol{w}_{I_2} = \{ w_3 \quad w_4 \}^{\text{T}}$, and $\boldsymbol{w}_S = \{ w_5 \quad w_6 \}^{\text{T}}$ are the vectors of displacements of the attaching points of each mount on the raft. Substituting Eq. (4) into Eq. (2) results in the following equation:

$$\boldsymbol{w}_b = \boldsymbol{Y}\left\{ \begin{array}{c} -\boldsymbol{K}_{I_1}\boldsymbol{R}_1^{\text{T}}\boldsymbol{x}_1 \\ -\boldsymbol{K}_{I_1}\boldsymbol{R}_1^{\text{T}}\boldsymbol{x}_2 \\ \boldsymbol{0} \end{array} \right\} - \boldsymbol{Y}\left\{ \begin{array}{c} \boldsymbol{K}_{I_1}\boldsymbol{w}_{I_1} \\ \boldsymbol{K}_{I_2}\boldsymbol{w}_{I_2} \\ \boldsymbol{K}_S\boldsymbol{w}_S \end{array} \right\} \tag{5}$$

For the rest of the system, the two machines are still considered as rigid bodies and excited by the external and internal forces introduced by the mounts of each machine simultaneously. Thus, the motion of the machines can be represented by

$$-\omega^2 \begin{bmatrix} \boldsymbol{Z}_{M_1} & 0 \\ 0 & \boldsymbol{Z}_{M_2} \end{bmatrix} \left\{ \begin{array}{c} \boldsymbol{x}_1 \\ \boldsymbol{x}_2 \end{array} \right\} = \left\{ \begin{array}{c} \boldsymbol{q}_{M_1} \\ \boldsymbol{q}_{M_2} \end{array} \right\} + \begin{bmatrix} \boldsymbol{R}_1 & 0 \\ 0 & \boldsymbol{R}_2 \end{bmatrix} \left\{ \begin{array}{c} \boldsymbol{K}_{I_1}\left(-\boldsymbol{R}_1^{\text{T}}\boldsymbol{x}_1 - \boldsymbol{w}_{I_1}\right) \\ \boldsymbol{K}_{I_2}\left(-\boldsymbol{R}_2^{\text{T}}\boldsymbol{x}_2 - \boldsymbol{w}_{I_2}\right) \end{array} \right\} \tag{6}$$

where $\boldsymbol{Z}_{M_i} = \begin{bmatrix} m_i & 0 \\ 0 & J_i \end{bmatrix}$ ($i = 1, 2$) is the inertia matrix of the machines, in which m_i, J_i ($i = 1, 2$) are the masses and the

rotational inertias around the centers of the two machines. The excitation of each machine is assumed to be introduced by the rotational motion of an out-of-balance motor, which produces an equivalent vertical force and a moment for each machine that is assumed to be harmonic and at the same circular frequency ω. Here, $\boldsymbol{q}_{M_1} = \{ F_1 \quad F_1\sigma_1 \}^{\mathrm{T}} \mathrm{e}^{\mathrm{j}\omega t}$ and $\boldsymbol{q}_{M_2} = \{ F_2\mathrm{e}^{-\mathrm{j}\varphi} \quad F_2\sigma_2\mathrm{e}^{-\mathrm{j}\varphi} \}^{\mathrm{T}} \mathrm{e}^{\mathrm{j}\omega t}$ are the external force vectors generated by the two machines, where F_1 and F_2 are the amplitudes of the forces generated by the machines and σ_1, σ_2 are coordinate values of the excitation forces in each local coordinate system of the machines, which provide the moment excitation, and φ is the phase between the two out-of-balance sources, with the reference source being the source on mass A.

Equations (5) and (6) can be combined to indicate the displacement of each position to which the other components are attached as

$$\boldsymbol{w}_b = \left(\boldsymbol{I} + \boldsymbol{Y}\boldsymbol{K}_t + \boldsymbol{Y}\boldsymbol{T}_k\boldsymbol{T}_p\right)^{-1}(\boldsymbol{Y}\boldsymbol{T}_k\boldsymbol{P}_0)\boldsymbol{f} \tag{7}$$

where $\boldsymbol{K}_t = \begin{bmatrix} \boldsymbol{K}_{I_1} & \boldsymbol{0} & \boldsymbol{0} \\ \boldsymbol{0} & K_{I_2} & \boldsymbol{0} \\ \boldsymbol{0} & \boldsymbol{0} & K_S \end{bmatrix}$ is the stiffness matrix of the composite system; $\boldsymbol{P_0} = \begin{bmatrix} \boldsymbol{P}^{-1} & \boldsymbol{0} \\ \boldsymbol{0} & \boldsymbol{0} \end{bmatrix}$ where $\boldsymbol{P} = \begin{bmatrix} -\omega^2\boldsymbol{Z}_{M_1} + \boldsymbol{R}_1\boldsymbol{K}_{I_1}\boldsymbol{R}_1^{\mathrm{T}} & \boldsymbol{0} \\ \boldsymbol{0} & -\omega^2\boldsymbol{Z}_{M_1} + \boldsymbol{R}_1\boldsymbol{K}_{I_1}\boldsymbol{R}_1^{\mathrm{T}} \end{bmatrix}$, $\boldsymbol{T_k} = \begin{bmatrix} -\boldsymbol{K}_{I_1}\boldsymbol{R}_1^{\mathrm{T}} & \boldsymbol{0} & \boldsymbol{0} \\ \boldsymbol{0} & -\boldsymbol{K}_{I_1}\boldsymbol{R}_1^{\mathrm{T}} & \boldsymbol{0} \\ \boldsymbol{0} & \boldsymbol{0} & \boldsymbol{0} \end{bmatrix}$ and $\boldsymbol{T}_p = \begin{bmatrix} \boldsymbol{P}^{-1}\begin{bmatrix} \boldsymbol{R}_1\boldsymbol{K}_{I_1} & \boldsymbol{0} \\ \boldsymbol{0} & \boldsymbol{R}_2\boldsymbol{K}_{I_2} \\ & \boldsymbol{0} \end{bmatrix} & \begin{matrix} \boldsymbol{0} \\ \boldsymbol{0} \end{matrix} \end{bmatrix}_{6\times 6}$ are the transfer matrixes, and $\boldsymbol{f} = \begin{Bmatrix} \boldsymbol{q}_{M_1} \\ \boldsymbol{q}_{M_2} \\ \boldsymbol{0} \end{Bmatrix}$ is the external force vector.

The natural frequencies of the composite system can be determined easily by the solution of

$$\left|\left(\boldsymbol{I} + \boldsymbol{Y}\boldsymbol{K}_t + \boldsymbol{Y}\boldsymbol{T}_k\boldsymbol{T}_p\right)^{-1}(\boldsymbol{Y}\boldsymbol{T}_k\boldsymbol{P}_0)\right| = 0 \tag{8}$$

Equation (7) can be expanded to general situations by adding the number of submatrices according to the number of machines. The transfer function matrix $\boldsymbol{Y}$, which presents the structural characteristics of an Euler–Bernoulli beam, can also be changed to a transfer function matrix of other types of beam or even a 2D structure.

2.2 Cost Function Definition and Choice of Vibration Control

A possible requirement for vibration control may be the reduction of the transmitted forces though the isolations of the raft. This condition would suggest reducing the motions at the attaching points.

To describe the motion of the raft for subsequent comparison of the response under different synchrophase situations, a suitable cost function can be given as

$$J = \dot{\boldsymbol{w}}_b^{\mathrm{H}}\dot{\boldsymbol{w}}_b \tag{9}$$

for which $\dot{w}_b$ is the vector of the velocities of the raft at the points where external components are attached and the superscript H denotes the Hermitian transpose. Thus, the cost function J becomes the sum of the squares of the modulus of the velocities. Substituting Eq. (7) into Eq. (9) results in

$$J = -\omega^2\boldsymbol{f}^{\mathrm{H}}\boldsymbol{\alpha}^{\mathrm{H}}\boldsymbol{\alpha}\boldsymbol{f} \tag{10}$$

for which $\boldsymbol{\alpha} = (\boldsymbol{I} + \boldsymbol{Y}\boldsymbol{K}_t + \boldsymbol{Y}\boldsymbol{T}_k\boldsymbol{T}_p)^{-1}(\boldsymbol{Y}\boldsymbol{T}_k\boldsymbol{P}_0)$ is the receptance matrix between the six connection points and the external forces acting upon the two machines.

Eq. (10) can be rewritten as

$$J = \boldsymbol{\Phi}^{\mathrm{H}}\boldsymbol{\Gamma}^{\mathrm{H}}\boldsymbol{\Gamma}\boldsymbol{\Phi} \tag{11}$$

where $\boldsymbol{\Gamma} = \mathrm{j}\omega\boldsymbol{\alpha}\boldsymbol{A}$ and $\boldsymbol{A} = \begin{bmatrix} F_1 & 0 & 0 & 0 & 0 & 0 \\ 0 & F_1\sigma_1 & 0 & 0 & 0 & 0 \\ 0 & 0 & F_2 & 0 & 0 & 0 \\ 0 & 0 & 0 & F_2\sigma_2 & 0 & 0 \\ 0 & 0 & 0 & 0 & 0 & 0 \\ 0 & 0 & 0 & 0 & 0 & 0 \end{bmatrix}$ are the amplitude of the forces present, while the phase of the forces is given by $\boldsymbol{\Phi} = \{ \boldsymbol{1} \quad \boldsymbol{1} \quad \mathrm{e}^{-\mathrm{j}\varphi} \quad \mathrm{e}^{-\mathrm{j}\varphi} \quad \boldsymbol{1} \quad \boldsymbol{1} \}^{\mathrm{T}}$. In this case, as the transfer function matrix $\boldsymbol{\Gamma}$ is independent of the phase between the forces introduced by the machines, determining the optimum phase angle φ_{op} of the secondary source with respect to the primary source at a certain frequency or working conditions is easy.

3 Numerical Simulations

This section aims to determine the influence of the phase angle between the two machines and the effect of the position of the secondary machine.

3.1 Performance of Synchrophasing

For numerical simulations and results, the following parameters are assumed: $m_1 = 2.2$ kg, $m_2 = 1.75$ kg, $m_b = 8.4$ kg, $L = 1.2$ m, $l_1 = 0.25$ m, $l_2 = 0.2$ m, $x_1 = 0.05$ m, $x_2 = 0.7$ m, $k_1 = k_2 = k_3 = k_4 = 2.34 \times 10^4$ N/m, and $k_5 = k_6 = 1.94 \times 10^4$ N/m.

The rotational inertia of the two machines are consequently calculated to be $J_1 = 0.0115$ kg·m^2 and $J_2 = 0.0058$ kg·m^2. In this particular case, the two machines are on opposite sides of the center of mass of the raft.

The numbers can be directly substituted into Eq. (8) to calculate the 10 resonance frequencies denoted by ω_n, which are shown in Table 1, compared with the results of finite element method (FEM). The corresponding mode shapes of the system are shown in Figs. 4a–j, in which the dash lines indicate the original position of the raft and machines while the modal deflection shapes are represented by the solid line.

For the resonance frequencies, a good agreement is observed between the analytical and FEM models. The difference is less than 2%, which gives confidence in the analysis used in this paper.

As shown in Fig. 4, the fundamental mode of the system is mainly the vertical displacement of the raft while the second mode involves rotation of the raft. The third and fourth modes are primarily the vertical displacements of the machines and the rotation of the raft with different rotation centers. The fifth and sixth modes involve only the rotation of each machine, which means that for these two particular modes, the forces introduced by the machines may not affect the motion of the raft. At the seventh and higher-order natural frequencies, the modes of the composite system are basically the bending modes of the raft as shown in Figs. 4g–j.

For the simulations, the force and moment introduced by machine A are considered as the reference excitation, and the forces generated by machine B are the control sources. In addition, because the machines are of rotary type, in which the imbalance leads to excitation, the magnitudes of the forces are proportional to the square of the rotational speeds of the machines, and the moment amplitudes are products of the forces and coordinate values of the sources around the machine mass centers. Therefore, in the numerical simulations, we can assume that the magnitudes of forces F_1 and F_2 are proportional to $3\omega^2$ and $2.5\omega^2$, respectively, and the coordinate values are 0.2 m and 0.15 m, respectively. The loss factor, which is assumed to be constant, is equal to 0.01.

A full search through the phase angle from 0° to 360° in step size of 3.6° (0.02π) was conducted to determine the optimum phase angle between the two machines to minimize or maximize the value of the cost function in the frequency band of 1 Hz to 1 kHz, which covers the first six rigid-body resonances and the first four flexural resonances. Figure 5a shows the minimum and maximum values of the cost function and Fig. 5b presents the phase angle.

As shown in Fig. 5a, the minimum (blue solid line) and maximum (red dash line) of the cost function and Fig. 5b indicates the corresponding phase angles. The blue circles show the phase that minimizes the cost function and the red squares show the phase that maximizes the cost function. As shown in Fig. 5a, a considerable reduction occurs in the frequency range from 0 to 1 kHz, especially at the first two rigid bodies and the third and fourth flexural natural frequencies. The reduction can be up to 25 dB. In Fig. 5b, the phase angle, either to minimize or maximize the cost function between the reference source and the control source, is either 0° or 180°, respectively.

Comparing Figs. 5a and b, we can observe that the phase angle to minimize or maximize the cost function shifts from 0° to 180° or vice versa at the frequencies of approximately 11.2, 30.5, 39.5, 44.1, 51.6, 362, and 731.5 Hz. Moreover, the difference between the minimum and maximum of the cost function at these frequencies is quite small, which means that around these particular frequencies, changing the phase of the two machines would not make much difference to the value of the cost function.

The main reason for the phase-change is that two different dominant mode shapes require an opposite phase angle to minimize the cost function at the two sides of these frequency points in the frequency axis. For instance, at the first phase-change frequency ($f_{c1} = 11.2$ Hz), the translational and rotational motions of the raft are equally dominant. As the two sources are positioned at each end of the raft, changing the

Table 1 Comparison of natural frequencies obtained analytically with that using FEM

Mode No.	Analytical ω_n/Hz	FEM ω_n/Hz	Difference/Hz	Percentage difference/%
1	8.4	8.5	0.1	1.20
2	14.4	14.4	0	0
3	30.1	29.8	0.3	1.00
4	31.5	30.9	0.6	1.90
5	40.1	40	0.1	0.30
6	45.2	45.1	0.1	0.20
7	93.9	94.4	0.5	0.50
8	250.3	249.6	0.7	0.30
9	488	485.2	2.8	0.60
10	805.8	797.2	8.6	1.10

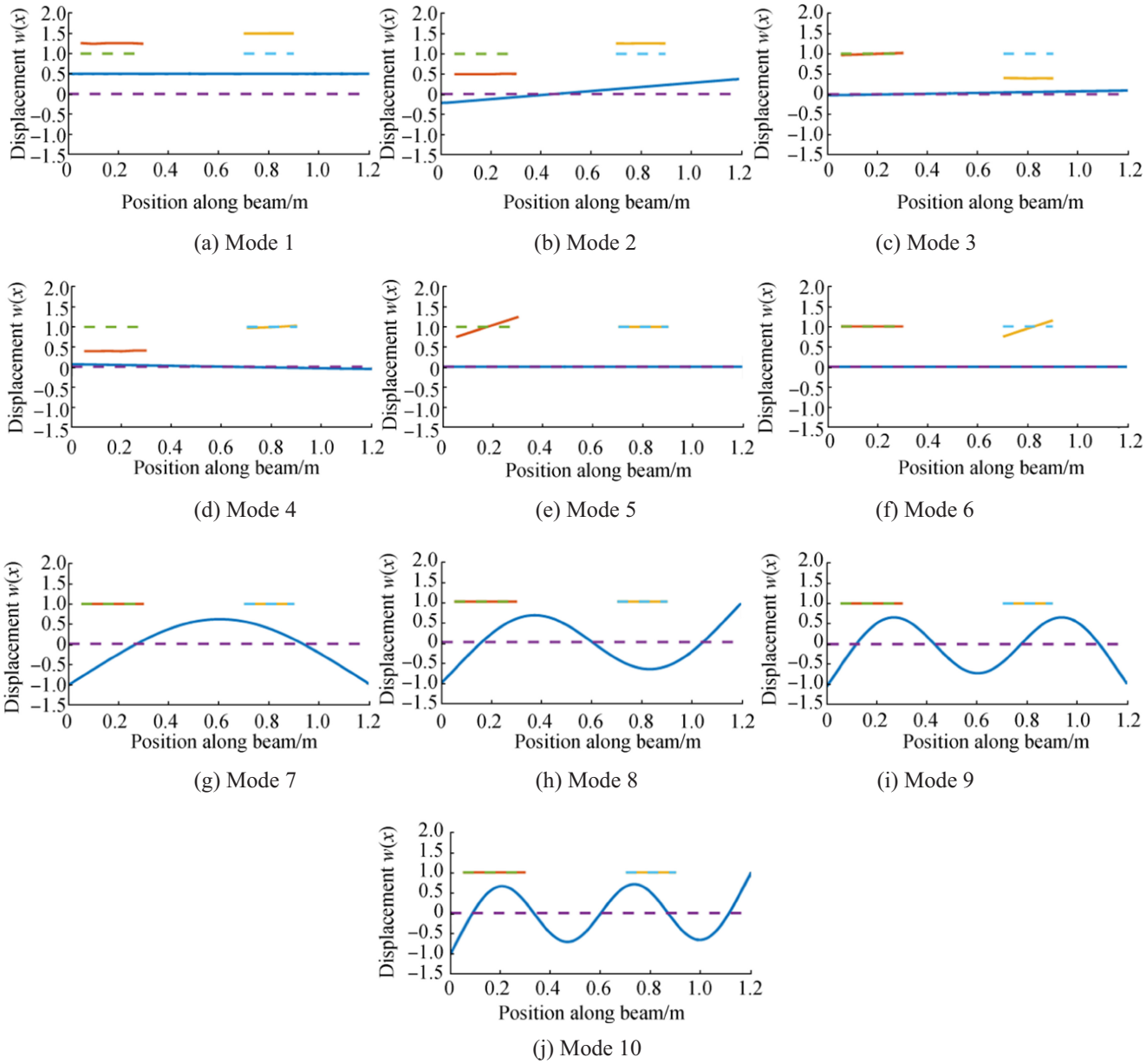

Fig. 4 Rigid-body modes and first four flexural modes of composite system

phase angle of the secondary source may reduce the vertical displacement of the raft but increase the rotation of the raft or vice versa.

Generally, the optimum phase angle depends on the number of nodal points between the machines. Depending on the moment, the two forces applied to the raft introduced by each machine are actually not equal to each other. Therefore, when the number of nodes between the dominant forces introduced by the machines is odd, the optimum phase is 180°, and the phase is 0° when the number is even.

For the third, fourth, and fifth changing points (f_{c3} = 39.5 Hz, f_{c4} = 44.1 Hz, and f_{c5} = 51.6 Hz), the dominant mode in the nearby frequency band is the rotation of one of the machines. Thus, energy is barely transmitted to the raft, as indicated in Fig. 5a, which shows that a small reduction of the cost function can be acquired in this frequency range. Thus, the changes in the optimum phase cannot lead to further reduction.

In fact, the sign of coordinate value of each excitation force indicates a different direction moment. In Figs. 6, 7, and 8, the cost functions and corresponding phase angles are shown when the coordinate value of each excitation force is changed.

As shown in Figs. 5a, 6a, 7a, and 8a, no significant difference exists among the maximum cost functions while the

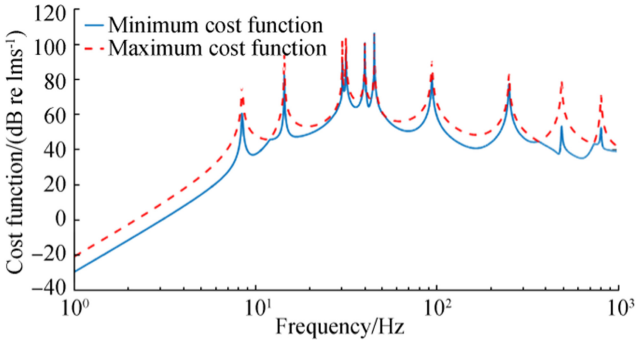

(a) Cost function

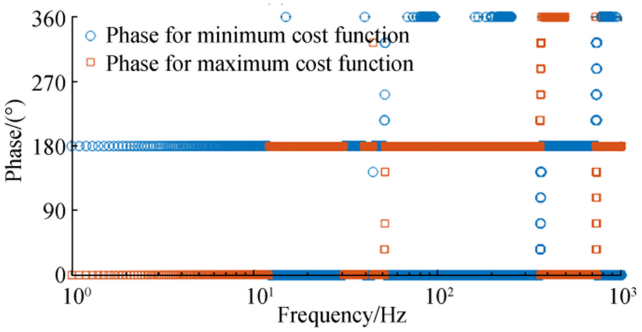

(b) Phase angle

Fig. 5 Plots of minimum (blue solid line) and maximum (red dash line) cost function and corresponding phase angles. The two locations of the excitation forces are 0.2 and 0.15, respectively

moments are in different directions. However, when the coordinate values of excitation forces are −0.2 and 0.15 m, an improved vibration control performance can be acquired especially at the second and seventh resonance frequencies. The reason is that altering the phase angle between the machines can reduce the vibration caused by the vertical forces and moments simultaneously. On the other hand, when the change of the phase reduces the vibration introduced by the forces but strengthens that caused by the moments, the synchrophasing does not achieve good vibration reduction.

More importantly, the optimum phase angles to reduce vibration vary under different situations. Apparently, the value of the optimum phase depends on the dominant part of the vibration caused by the forces or moments.

When the coordinate values of the two machines are set to 0, only forces generated by the machines act on the raft. The corresponding results are shown in Figs. 9a and b, which are similar to Figs. 5a and b.

A distinct difference in the cost function curve can be observed in the high-order resonances. As the fifth and sixth resonances of the system are the rotation modes of each machine, the motion of the raft becomes quite small because no moment is acting on it. According to the flexural mode of the raft, the two mounts of each machine are often located near or across flexural mode nodes. Thus, the vibration of such modes is not easily excited by the machines to a certain extent.

3.2 Effect of Position of Secondary Machine

Changing the position of machine B may affect the optimum phase to minimize the cost function if the mode shape and resonance frequency of the composite structure does not change greatly, especially in the high-frequency range. Figure 10 shows the changes in the optimum phase when the excitation frequency varies from 1 Hz to 1 kHz and the position of machine B, x_2, changes from 0.3 to 1 m. As shown in the figure, three values of the optimum phase angle are used to minimize the cost function, namely, 0°, 180°, or 360°, which are represented by blue, green, and yellow circles, respectively.

As shown in Fig. 10, the first phase-change frequency due to the first and second rigid-body resonance modes of the raft moves from 14.6 to 10.7 Hz as the position of machine B changes. The reason is that the frequency of the rotational rigid-body mode shifts to a lower frequency and the rotation center is still located between the two machines. The third and fourth resonance frequencies of the composite system also change slightly when the secondary machine moves, which

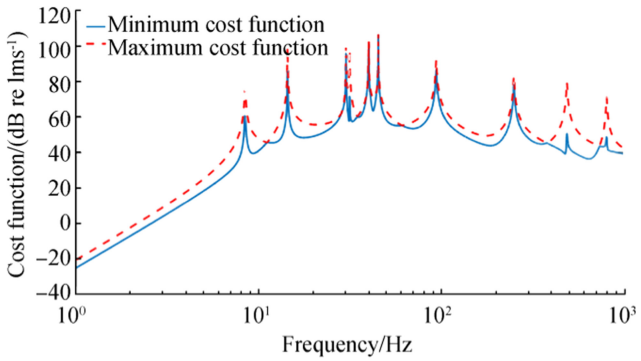

(a) Cost function

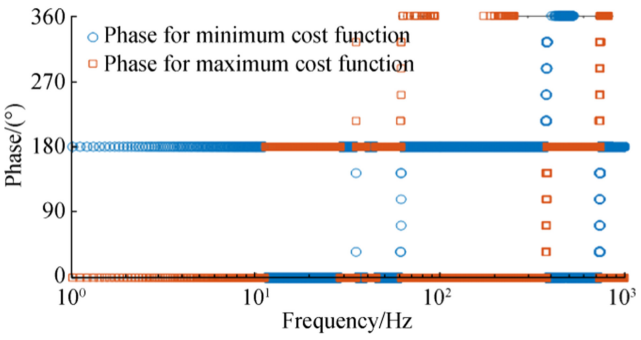

(b) Phase angle

Fig. 6 Plots of minimum (blue solid line) and maximum (red dash line) cost function and corresponding phase angles. The locations of the excitation forces are −0.2 and 0.15 m, respectively

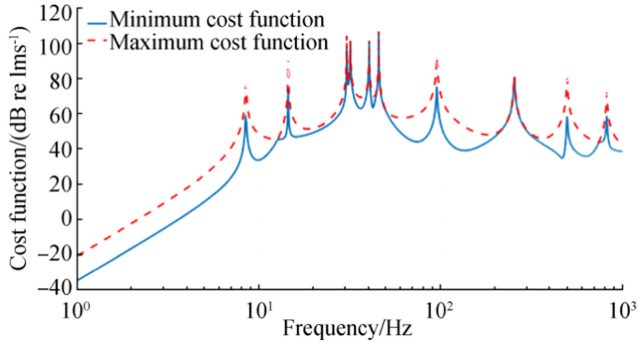

(a) Cost function

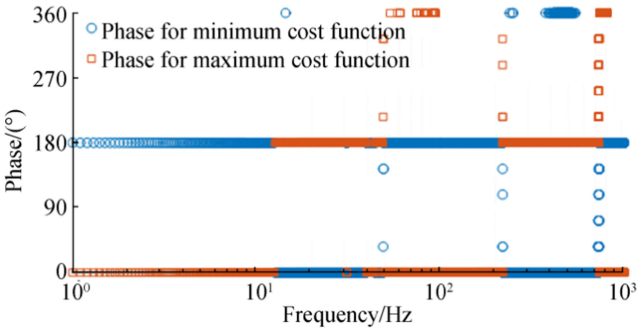

(b) Phase angle

Fig. 7 Plots of minimum (blue solid line) and maximum (red dash line) cost function and corresponding phase angles. The two locations of the excitation forces are 0.2 and − 0.15 m, respectively

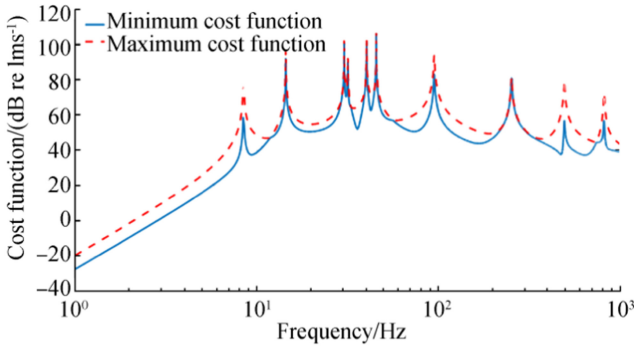

(a) Cost function

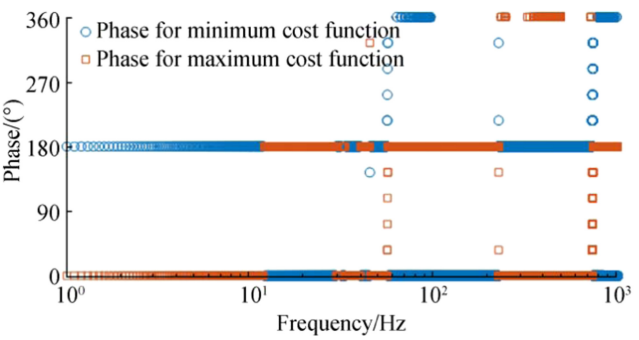

(b) Phase angle

Fig. 8 Plots of minimum (blue solid line) and maximum (red dash line) cost function and corresponding phase angles. The locations of the excitation forces are − 0.2 and − 0.15 m, respectively

leads to the shift of the frequency of the second phase-change frequency. However, the reason for the change in the optimum phase angle is the same as mentioned above.

The variety of machine B's position does not change the frequencies of the fifth mode and those at higher frequencies. Therefore, as the fifth and sixth modes of the system involve the rotation of the two machines, the motion of the raft is always insensitive to the adjustment of the phase of machine B in the 38–50 Hz frequency range.

Although the frequencies of the fifth and higher-order modes do not vary with the position change of machine B, the mode shape changes slightly especially the positions of the nodes, thereby eventually affecting the control phase angle. For the first bending mode of the raft, for which two nodes exist, the value of the optimum phase angle only changes once. As shown in Fig. 4g, when x_2 varies from 0.3 to 0.6 m, one of the nodes always occurs between the two mounts of machine A. A dominant force exists between the two forces introduced by each machine to the raft due to the action of the moment. Therefore, in this situation, the dominant force generated by machine A is on the same side of the nodal point with the forces introduced by machine B, which leads to the optimum value of the phase being 180°. On the other hand, when the x_2 changes from 0.6 to 1 m, the control phase is always 0°. Owing to changes in the position of machine B, the nodal points of the first bending mode of the raft changes, but a node always exists between the two dominant forces generated by the two machines.

When the motion of the raft mainly consists of the flexural bending, the optimum value of the phase angle basically depends on the number of nodes between the two machines, especially the dominant forces introduced by each machine due to the moment. For example, with an excitation frequency of 487 Hz, which is the third flexural resonance frequency, the optimum phase changes twice when the position of the secondary machine, x_2, varies from 0.3 to 1. In this situation, a total of four nodes exist, which are approximately located at 0.15, 0.4, 0.75, and 1.05 m. Therefore, between the two mounts of machine A, a node always exists, and a node is also between the mounts of machine B when x_2 changes from 0.3 to 0.5 m and from 0.85 to 1 m. Furthermore, the number of nodes between the two machines are 0 and 2, which means that the two pairs of attaching points of the machines are in anti-phase. Therefore, the optimum phase angle is 0° in these situations. Similarly, the motions of each pair of

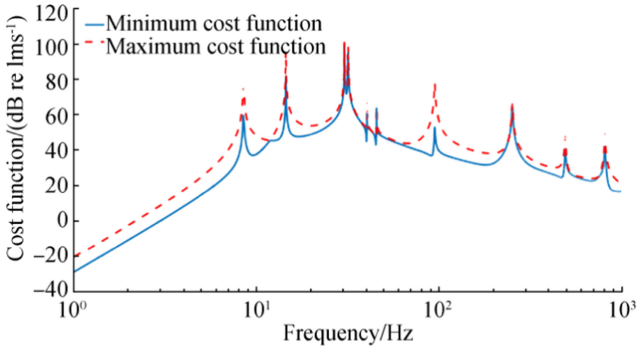

(a) Cost function

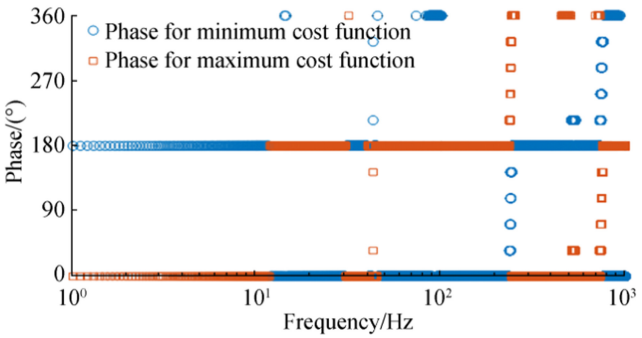

(b) Phase angle

Fig. 9 Plots of minimum (blue solid line) and maximum (red dash line) cost function and corresponding phase angles. The two locations of excitation forces are set to 0

connection positions are the same when x_2 varies from 0.5 to 0.85 m. Thus, the phase angle to minimize the cost function becomes 180°. In addition to these findings, two particular situations occur in which no node exists between the mounts of machine B when x_2 is around 0.5 m and 0.8 m. The value of the optimum phase angle then depends on the number of nodes between machine B and the dominant force generated by machine A. For 1 or 2 nodes, the optimum phase is 0° or 180°, respectively.

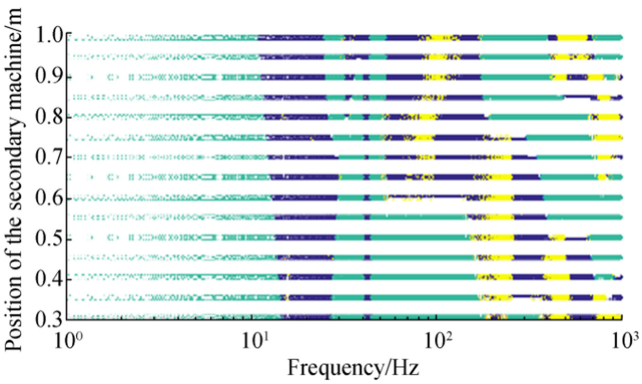

Fig. 10 Changes in optimum phase when excitation frequency varies from 1 Hz to 1 kHz and position of machine B, x_2, varies from 0.3 to 1 m

4 Conclusions

A study was conducted on synchrophasing vibration control on an aluminum extruded box section beam in which two rotary machines were each resiliently attached by two rubber mounts. This type of machinery installation is common in practice such as that on a ship. The 1D structure was chosen to represent the machinery raft because it would simplify the analysis when both forces and moments introduced by the machines were considered.

This study has demonstrated theoretically that adjusting the relative phase angle between the machines can reduce the cost function, which is the sum of the squares of velocities of attaching points on the raft at each frequency of interest. The phase angle needed to minimize the cost function is always 0° or 180°. Several frequencies exist at which the cost function does not vary with the change of phase angle between the machines because the dominant motion of the raft changes from one mode of the system to another. This condition occurs because changing the phase at these frequencies enhances one mode of the system and attenuates the other one or vice versa. Besides, the moment introduced by each machine can significantly affect the performance of synchrophasing and the optimum phase angle, especially when the moments are anti-phase with the force in-phase. The main reason is that altering the phase angle between the machines may not only reduce the vibration caused by the vertical forces but also enhance vibration caused by moments, which cannot be ignored in practice.

The numerical model has shown that altering the position of the secondary source may cause a slight change to the mode shape of the composite system, thereby changing the optimum phase between the two machines. At positions where the control phase changes from 0° to 180° or vice versa, the motion of the raft is insensitive to the variation of the phase angle of the secondary machine with respect to the primary machine.

Although these conclusions have been obtained from numerical results based on a 1D structure, they are also applicable to a general structure. However, when the structure is complex, the coupling of the factors of the excitations would be complex also.

References

Blunt DM, Rebbechi B, 2007. Propeller synchrophase angle optimisation study. Proceedings of the 13th AIAA/CEA Aeroacoustics Conference, Rome, Paper No. AIAA-2007-3584. https://doi.org/10.2514/6.2007-3584

Dench MR, Brennan MJ, Ferguson NS, 2005. Active control of the flexural vibration of a thin beam with free ends. Institute of Sound &

Vibration Research, Southampton, United Kingdom, ISVR Technical Memorandum No. 949

Dench MR, Brennan MJ, Ferguson NS (2013) On the control of vibrations using synchrophasing. J Sound Vib 332:4842–4855. https://doi.org/10.1016/j.jsv.2013.04.044

Efimtsov BM, Zverev AY (1992) Sound field produced in a shell by 2 synchrophased sources. Soviet Physics Acoustics-USSR 38(4):382–386

Fuller CR, Elliott SJ, Nelson PA (1997). Active control of vibration. Academic Press Ltd, Cambridge, USA, 30–33

Fuller CR (1986) Analytical model for investigation of interior noise characteristics in aircraft with multiple propellers including synchrophasing. J Sound Vib 109(1):141–156. https://doi.org/10.1016/S0022-460X(86)80028-1

Fu J, Wang YS, Wei YS (2012) Analysis of power flow of floating raft with multi-exciters by FEM. J Ship Mech 16(6):684–691. https://doi.org/10.3969/j.issn.1007-7294.2012.06.008

Harada I (1977). Blower noise reducing method by phase control. Patent No. JP54060656

Howard C (2004). Experimental results of synchrophasing two axial fans in a duct. Proceedings of 2004 International Symposium on Active Control of Sound and Vibration, Williamsburg, USA, Paper No. A04_29

Huang X, Wang Y, Sheng L (2015) Synchrophasing control in a multi-propeller driven aircraft. *2015 American Control Conference*. Chicago, USA, 1836–1841

Jones JD, Fuller CR (1986) Noise-control characteristics of synchrophasing I experimental investigation. AIAA J 24(8):1271–1276. https://doi.org/10.2514/3.9392

Li ZG (2015) Computation and analysis of the isolation performance of floating rafts and double-stage vibration isolation systems. Noise Vibration Control 35(6):65–68. (in Chinese). https://doi.org/10.3969/j.issn.1006-1335.2015.06.014

Magliozzi B (1995). Adaptive synchrophaser for reducing aircraft cabin noise and vibration. U.S. Patent 5453943

Mallock A (1905) A method of preventing vibration in certain classes of steamships. Trans Instit Naval Architects 47:227–230

Pla FG, Goodman GC (1993). Method and apparatus for synchronizing rotating machinery to reduce noise. U.S. Patent 5221185

Pla FG (1998). Method for reducing noise and/or vibration from multiple rotating machines. U.S. Patent 5789678

Song YC, Yu HL (2008) Research of effect of isolation system's location and excited phase on vibration response of foundation. Noise Vibration Control 28(5):33–35. (in Chinese). https://doi.org/10.3969/j.issn.1006-1355.2008.05.007

Yang TJ, Zhang XY, Xiao YH, Huang JE, Liu ZG (2004) Adaptive vibration isolation system for marine engine. J Mar Sci Appl 3(2):30–35. https://doi.org/10.1007/BF02894330

Yang TJ, Huang D, Li XH, Brennan MJ, Zhou LB, Zhu MG, Liu ZG (2018) Vibration control of a floating raft system by synchrophasing of electrical machines: an experimental study. J Vib Acoust 140(4):041015. https://doi.org/10.1115/1.4039407